International Journal of Nanoelectronics and Materials

In Press, Accepted Manuscript – Note to user

Analysis on Sound Absorber Panel Made of Oil Palm Mesocarp Fibre using Delany-Bazley and Johnson-Champoux-Allard Models

Hanif Abdul Latif[1], Izzuddin Zaman[2*], Musli Nizam Yahya[2], Mathan Sambu[3] and Qingshi Meng[4]

[1]SI Acoustic Sdn Bhd, Jalan Bulan, U5/168 Seksyen U5, Bandar Pinggiran Subang, 40170 Shah Alam, Selangor, Malaysia
[2]Mechanical Failure Prevention and Reliability Research Centre, Faculty of Mechanical and Manufacturing Engineering, Universiti Tun Hussein Onn Malaysia, 86400 Batu Pahat, Johor, Malaysia
[3]Department of Mechanical Engineering, Faculty of Engineering and Technology, Nilai University, 71800 Nilai, Negeri Sembilan, Malaysia
[4]School of Engineering, Mawson Lakes Campus, South Australia 5095, Australia

ABSTRACT

Oil palm mesocarp fibre is seen as one potential of reinforcement in polymers due to its high strength, low cost, environmentally friendly nature and availability. Recently, it has attracted greater interest from academia and industries due to its potential for making a low-cost sound absorption panel. Therefore, this study was obliged to investigate the acoustic characteristics and the physical properties of oil palm mesocarp fibre (OPMF) as a porous material for sound absorbing panel. The measurements of the sound absorption coefficient were determined by using: (1) analytical model of Delany-Bazley, (2) analytical model of Johnson-Champoux-Allard, and (3) experimental of the impedance tube method. A commercial polyurethane (PU) was used as a composite binder during the intermixing process with the fibres. The manufacturing parameters were 10/90, 20/80, 30/70 and 40/60 by wt.% of PU/OPMF. The outcome shows that adding binder compacts the fibre by reducing the pore diameter and porosity, thus increases flow resistivity. Results also indicated that Johnson-Champoux-Allard model can justify the overall trend of absorption coefficient perfectly in contrast to Delany-Bazley model. Overall, OPMF with 10 wt.% PU binder displayed greater absorption from low to mid-frequency range and the highest value of noise reduction coefficient of 0.66, while fibres with 20 wt.% PU produce the highest value of sound absorption coefficient of 0.99 at 1000 Hz. The results conclude that oil palm mesocarp displays potential and brighter prospect to be implemented as a sound absorption panel as demonstrated in this study.

Keywords: Delany-Bazley model, Johnson-Champoux-Allard model, noise reduction coefficient, oil palm mesocarp fibre, porous material, sound absorption coefficient

1. INTRODUCTION

Malaysia in present is one of the largest producers and exporters of palm oil in the world. It was estimated approximately 48.5% of total planted area hectares in Peninsular Malaysia and about 51.5% in Sabah and Sarawak [1]. Due to the aggressive growth in planting, harvesting and mill operations, the country produces an enormous quantity of oil palm residues such as oil palm frond (OPF), oil palm shell (OPS), oil palm trunk (OPT), oil palm empty fruit bunches (OPEFB) and oil palm mesocarp fibre (OPMF) [2]. Even though these materials are considered wastes, some of them such as OPMF has shown potential as an alternative material for glass and other synthetic fibres. This is coupled with a growing global awareness of environmental, ecological and health issues caused by synthetic materials that drive the use of natural based materials as valuable products.

In Malaysia primarily, Forest Research Institute of Malaysia (FRIM) and Malaysian Palm Oil Board (MPOB) has conducted fundamental researches to find the potential of using oil palm residues as ~~raw material in diverse engineering app~~lications particularly in automotive components, building

*izzuddin@uthm.edu.my

materials and aerospace industry [3–5]. In recent years, there have been an increasing interest studies on utilizing oil palm mesocarp for producing valuable chemical products by applying a thermochemical conversion process [6,7], hydrothermal pre-treatment [8,9] and combustion of biomass [10]. However, to the best knowledge of authors, the study related to OPMF's sound performance or sound absorption behaviour has yet to be performed so far.

These days, noise has turned out to be one of many factors that influence human health and environment due to the advancement of modern industry and traffic system. Hence, the need for effective techniques for reducing noise has become a major issue, and the latest is using waste material and natural fibres as a sound absorber. This is because the use of these materials not only has potential can reduce noise, but also able to solve environmental pollution problems. For example, several researchers have succeeded in developing agricultural waste to produce sound absorption panels. Yang et al. [11] studied the possibility of using rice straws and waste tires as sound insulation board and they found that the acoustical insulation of composite panel was superior to other wood-based panel products. Meanwhile, Berardi and Iannace [12] examined the acoustical characterization of several natural fibres such as kenaf, wood, hemp, coconut, cork, cane, cardboard, and sheep wool.

Some of the researchers also mixed the raw material with an adequate binder or adhesive to create a solid sample of the sound absorber, even though this is not considered a new method in the polymer composite. For instance, Nor et al. [13] reported that by applying the binder can improve the acoustic properties especially in the high-frequency range. Maderuelo-Sanz et al. [14] demonstrated that the sample porosity decreases when the percentage of polyurethane (PU) binder increases, thus enhance the acoustic flow resistivity. Furthermore, Borlea et al. [15] mixed the pine sawdust with commercial PU binder with two different weight percentages 20% and 30% and found that sample with 30 wt.% improves acoustic properties better than 20 wt.% of PU binder in a low-frequency range. However, 20 wt.% shows the highest sound absorption coefficient of 0.9 at a high-frequency range between 3150 – 6300 Hz.

In spite of these studies, there is still little knowledge about sound absorption behaviour of waste materials, in particular to OPMF. Therefore, this study is devoted to investigating the potential use of OPMF in acoustic absorption application. The effect of binder in determining the optimum acoustic performance (e.g. sound absorption coefficient and noise reduction coefficient) was analysed in this research, including the physical properties measurement such as flow resistivity, tortuosity, porosity, and characteristic length. In order to better understand the sound absorption properties of OPMF, the experimental results were validated with the analytical prediction models of Delany-Bazley and Johnson-Champoux-Allard.

2. MATERIAL SELECTION AND PREPARATION

2.1 Raw material

Oil palm mesocarp fibres were provided by Oil Palm Processing Sdn. Bhd., Kluang, Johor, Malaysia. The raw fibre consists of a mixture of the outer skin (exocarp), shell (endocarp), crushed kernel and mesocarp. Prior to sample preparation, the mesocarp fibres were undergoing several pre-treatment processes to remove unwanted dirt and materials such as kernels and

endocarp. This includes by soaking the fibres in clean water for one week before being dried naturally under the sun and then heated in the oven at 70 ºC for 4 hours in order to remove residual water. The cleaned fibres were finally cut using a crusher machine into 10–15 mm length as shown in Figure 1. The fibers were then milled by rotor mill machine to get fine sizes random fibers before were sieved using a sieve shaker machine with seize ring 200 µm to obtain uniform size of the filler. Meanwhile, polyol and isocyanate were purchased from Dwicira Resources Sdn. Bhd. in order to form polyurethane (PU) binder.

Figure 1. Oil palm Mesocarp fibre with 10-15 mm length.

2.2 Sample preparation

There were four weight percentages of PU binder prepared with OPMF in this research, which range from 10 to 40 wt.%. At ratio 0.5 of isocyanate to polyol were dropped into arrays of OPMF, followed by stirring for 10 minutes to achieve homogeneous dispersion. The mixture was then transferred into the cylindrical moulds of 28 mm and 100 mm diameters with a thickness of 50 mm, and later curing at room temperature for 24 hours. The large diameter OPMF/PU sample is for the low-frequency test and the small diameter sample is for the high-frequency test.

3. METHODS

3.1 Experimental measurement using impedance tube

There are two parameters were measured in this research to investigate the acoustical properties of porous absorbent; the sound absorption coefficient and noise reduction coefficient (NRC). The impedance tube method was implemented to investigate these acoustical properties. The impedance tube comprises two different tubes of 28 mm and 100 mm diameters, two 1/4 inch pressure microphones type GRAS-40BP, preamplifier, and two channels data acquisition system 01dB which connected to software SCS8100. This tube configuration represents the basis, standard system setup for sound absorption coefficient and impedance measurements. The microphones location is established based on the standard method, by calculating the transfer function of two fixed microphones which are located at two different positions in the tube wall. The calibrator used for microphone sensitivity was Larson Davis CAL 200. The test was performed according to ISO 10534-2, where the measurement of sound absorption properties of the material was based on the two microphones transfer-function method. The set up for the impedance tube measurement system used in the laboratory work is illustrated in Figure 2.

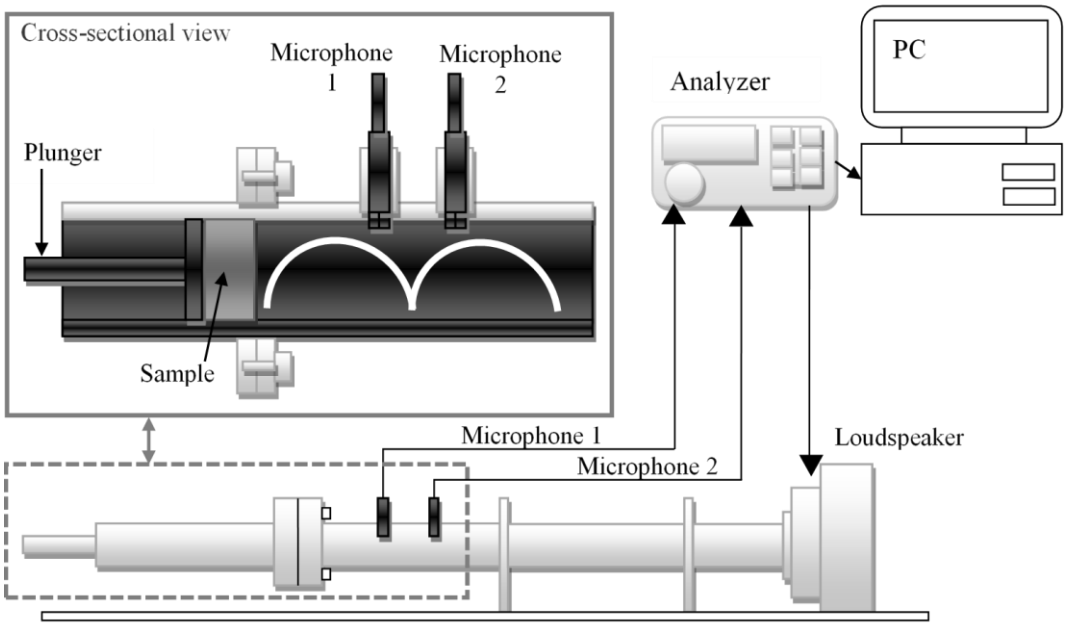

Figure 2. Schematic sketch of impedance tube setup

Noise reduction coefficient, on the other hand is a single number rating system for indexing the ability of material to absorb sound. It is measured based on the average value of sound absorption coefficient over human speech frequencies range at 250, 500, 1000, and 2000 Hz [16]. The NRC can be calculated using Equation (1), where α is the sound absorption coefficient.

$$NRC = \frac{\alpha_{250Hz} + \alpha_{500Hz} + \alpha_{1000Hz} + \alpha_{2000Hz}}{4} \quad (1)$$

3.2 Delany-Bazley model

In this section, an empirical formula based on Delany-Bazley model (DBM) was utilized for the estimation of characteristic impedance and propagation coefficient of oil palm mesocarp fibres. The model was considered very simple and easy approximation to the solution as it uses only frequency and flow resistivity parameter which are an intrinsic property of the material [17,18].

The characteristic of impedance Z_c can be obtained by:

$$Z_c = \rho_0 c_0 F_1(X) \quad (2)$$

And the wavenumber, k by:

$$k = \frac{2\pi f}{c_0} F_2(X) \quad (3)$$

Where ρ_0 is the density of air, c_0 and f are speed and frequency of sound. While, $F_1(X)$, $F_2(X)$ and X are given in Equations (4)–(6), respectively:

$$F_1(X) = 1 + 0.0571X^{-0.754} - j0.087X^{-0.732} \quad (4)$$

$$F_2(X) = 1 + 0.0978X^{-0.700} - j0.189X^{-0.595} \quad (5)$$

$$X = \frac{\rho_0 f}{\sigma} \quad (6)$$

Where σ the flow resistivity of the fibrous material and j is an imaginary number. This model is only applicable when the boundary of X falls in the range of $0.01 < X < 1.0$, and the flow resistivity measurement in the range of $1000 \leq \sigma \leq 50000\ Nsm^{-4}$. Thus, frequency dependent sound speed, c_{eq} and density of a highly porous material, ρ_{eq} according to this model can be expressed as follows:

$$c_{eq} = \frac{\omega}{k} = \frac{c_0}{F_1(X)} \quad (7)$$

$$\rho_{eq} = \frac{Z_c}{C_{eq}} = \frac{Z_c k}{w} = \rho_0 F_1(X) F_2(X) \quad (8)$$

As mentioned earlier that this approach only depends on frequency and flow resistivity to study the behaviour of porous materials, so it might not be expected to provide the perfect predictions [19].

3.3 Johnson-Champoux-Allard model

This model is devoted to the semi-phenomenological theoretical model of porous absorbents. Several researchers have been engaged in generating of the model where models of Allard and Atalla [19], Champoux and Allard [20] and Johnson *et al.* [21] were combined to produce a simple phenomenological model. There are two parameters required in this model which are the effective density, ρ_e and the effective bulk modulus of air in the material, K_e. Both can be expressed in the following Equations (9) and (10), respectively:

$$\rho_e = k_s \rho_0 \left[1 + \frac{\sigma \varepsilon}{j\omega \rho_0 k_s} \sqrt{1 + \frac{4jk_s{}^2 \eta \rho_0 \omega}{\sigma^2 \Lambda^2 \varepsilon^2}} \right] \quad (9)$$

$$K_e = \frac{\gamma P_0}{\gamma - (\gamma - 1) \Bigg/ \left(1 + \frac{8\eta}{j\Lambda'^2 N_P \omega \rho_0} \sqrt{1 + \frac{j\rho_0 \omega N_p \Lambda'^2}{16\eta}} \right)} \quad (10)$$

Where k_s, ε, Λ and Λ' are the tortuosity, porosity, viscosity and thermal characteristic length of porous material, respectively; ω is angular frequency, η is the viscosity of air, γ is the ratio of specific heat capacity for air (≈ 1.4) and P_0 is atmospheric pressure. The Prandtl number, N_p can be calculated from Equations (11)–(13):

$$N_p = \left(\frac{\delta_v}{\delta_h} \right)^2 \quad (11)$$

$$\delta_v = \sqrt{\frac{2\eta}{\rho\omega}} \tag{12}$$

$$\delta_h = \sqrt{\frac{2\eta\kappa}{\rho c_p \omega}} \tag{13}$$

Where δ_v and δ_h is the thickness size of the viscous and thermal boundary layer, respectively; κ is the thermal conductivity of air and c_p is the specific heat capacity of air at constant pressure. In this study, the fibre structure was assumed as elastic cylindrical fibres and the layer of porous material with identical parallel pores was considered perpendicular to the surface (normal incidence). After determining the Equations (9) and (10), the characteristic impedance, Z_c and the complex wave number, k in a pore can be determined by:

$$Z_c = (K_e \rho_e)^{1/2} \tag{14}$$

$$k = \omega(\frac{\rho_e}{K_e})^{1/2} \tag{15}$$

3.4 Flow resistivity measurement

The flow resistivity of the samples was measured using the formulation that developed by Ballagh [22]. Based on the derived formulation, there is a close relationship between flow resistivity, density, and fibre diameter. For this study, Equation (16) was implemented to determine the flow resistivity, σ.

$$\sigma = 490 \frac{\rho_{bulk}^{1.61}}{d_{fibre}} \tag{16}$$

Where d_{fiber} is diameter fibre and ρ_{bulk} is bulk density. Each fibre is assumed as a perfect cylindrical shape. Here, the fibres were taken randomly and the diameter fibres were measured by using a digital microscope scan. On the other hand, the bulk density was measured experimentally via porosity measurement.

3.5 Porosity measurement

The porosity, ε of each sample can be determined by using Equation (17) by measuring two variables which are pore volume, V_p and bulk volume, V_b.

$$\varepsilon = \frac{V_p}{V_b} \tag{17}$$

$$V_p = \frac{(W_s - W_d)}{\rho_s} \tag{18}$$

$$V_b = \frac{W_s - W_i}{\rho_s} \tag{19}$$

Where W_s is the weight of the saturated sample, W_d is the weight of the dried sample, W_i is the weight of the immersed sample and ρ_s is the density of the saturated liquid. In this experiment, the weight of the dried sample was measured in a vacuum condition in order to produce a more accurate result [23].

3.6 Tortuosity measurement

Tortuosity is linked to the inertial part of the force between fluid and frame. There are various methods to get the tortuosity accurately but in order to avoid samples getting damaged from the soaking process, the tortuosity, k_s was measured by using Equation (20) according to Umnova *et al.* [24].

$$k_s = \frac{1}{\sqrt{\varepsilon}} \tag{20}$$

3.7 Characteristic lengths measurement

In this study, the viscous characteristic length can be found using the empirical equation defined by Allard and Atalla [19]. The fibres are assumed to lie in planes parallel to the surface of the layers and the macroscopic air velocity is perpendicular to the direction of the fibres at normal incidence. The fibres are also assumed as an infinitely long cylinder having a circular cross-section with a known radius. The viscosity characteristic length, Λ is given by:

$$\Lambda = \frac{1}{2\pi r l} \tag{21}$$

Where r and l are the radius and total length of the fibre, respectively. The total length of fibre can be calculated from the following equation:

$$l = \frac{1}{\pi r^2 \left(\frac{\rho_{bulk}}{\rho_{fibre}}\right)} \tag{22}$$

Where ρ_{fibre} is the density of the fibre. The thermal characteristic length was evaluated from Equation (23).

$$\Lambda' = 2\Lambda \tag{23}$$

4. RESULT AND DISCUSSION

4.1 Physical properties within porous absorbents

Average values of the physical properties of the OPMF samples are tabulated in Table 1. Obviously, it can be seen that different percentage of PU and OPMF contents produces variation in their physical properties. Large differences observed in flow resistivity demonstrate the significant effect of PU binder on the bulk density and diameter of produced fibres [22,25]. The range of flow resistivity, calculated using Ballagh formula for the porous material is obtained from 15,000 to 37,000 Nms^{-4} as shown in Table 1. With the exception of pure OPMF sample, the flow

resistivity gradually increases with the increase of the PU binder concentration for combined mixture with OPMF particle size ranging from 200 microns to 1 mm [26]. Meanwhile, as expected the porosity of OPMF with 40 wt.% PU binder shows the lowest value followed by 30 wt.%, 20 wt.% and 10 wt.% PU binder. This is because the binder compacts the fibre tightly causing less of hollow space within the fibre composite [27]. Figure 3 illustrates the relationship between the porosity and flow resistivity where reducing the porosity results in an increased flow resistivity.

TABLE 1 Effect of PU binder on physical properties of OPMF

Sample OPMF with PU loading (wt.%)	Flow Resistivity (Nms^{-4})	Porosity	Tortuosity	Viscous characteristic length (μm)	Thermal characteristic length (μm)
0	37,415.52	0.847	1.087	97.81	195.62
10	17,201.09	0.882	1.065	582.37	1164.74
20	17,566.14	0.801	1.117	613.73	1227.46
30	18,594.63	0.766	1.143	629.27	1258.54
40	21,439.48	0.639	1.251	700.15	1400.3

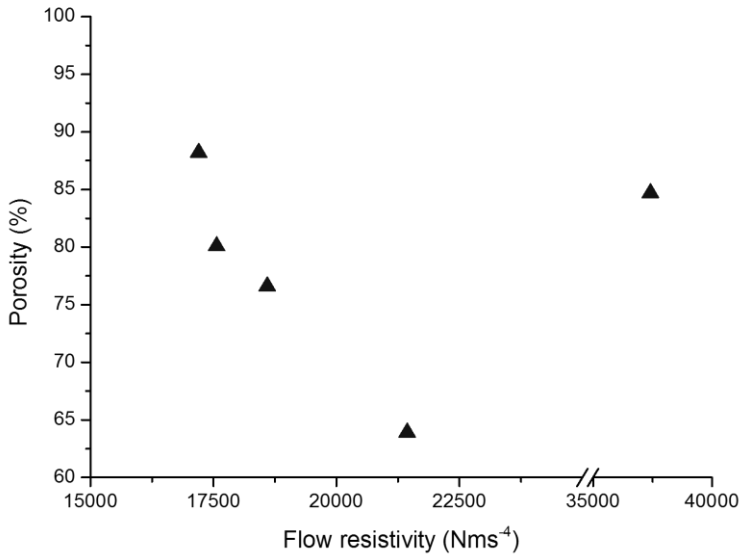

Figure 3. The porosity as a function of the flow resistivity for OPMF samples.

On the other hand, the PU binder is also found influencing the average path length of a pore and thereby give higher tortuosity. This is due to the random arrangement of fibres creating more tortuosity but reducing pores that may affect the acoustical performance [28]. The range of the tortuosity is from 1.087 to 1.251. In similar cases, the characteristic lengths were found increased for both viscous and thermal, by increasing the loading percentage of binder. These outcomes indicate that the binder affects the radius of the pores and the stiffness of the material.

4.2 Acoustical properties

Figure 4 shows that the sound absorption coefficient against frequencies spectra for OPMF samples with different percentages of PU binder as measured by impedance tube. It was found

that the absorption coefficients for most of OPMF samples initially increase from 0.1 to ~0.9 but then decrease to ~0.7 at between 1000 Hz to 3000 Hz before reach maximum peak of ~1 at 4000 Hz. Basically, the sound absorption spectra obtained are in good agreement with the previously published data where it shows a standard pattern for porous absorbent material [16,29]. The result indicated that all OPMF samples demonstrated higher sound absorption coefficient at the medium to high-frequency range with the average of absorption above 0.7.

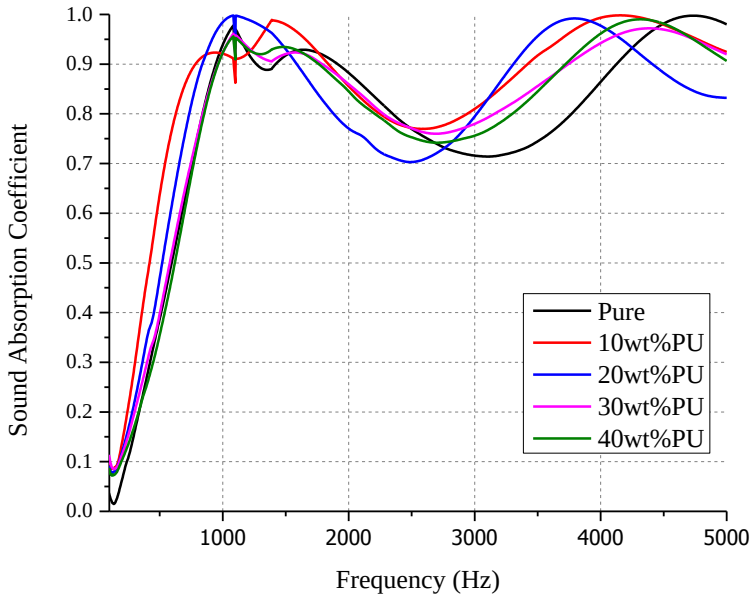

Figure 4. Variation of sound absorption coefficient of OPMF at different PU concentration.

The best acoustic performance over the frequency range of interest is obtained for the sample OPMF with 10 wt.% PU binder. For this sample, the maximum values of the sound absorption coefficient are 0.96 and 0.98, respectively achieved at the frequency of 1400 Hz and 4100 Hz. This is attributable to the high porosity obtained by the sample of 0.882. However, the sample with 20 wt.% PU binder displays the highest value of sound absorption of 0.99 at 1000 Hz. This result demonstrated that the OPMF sample with low concentration PU binder which in this case is below than 20 wt.% can improve sound absorption at the medium frequency range, thus indicates the cavity resonances were suppressed by damping of fibre causing loss of sound energy via friction with the pore walls [28]. In addition, the PU binder also contributes to the improvement in the low to medium frequencies because of the membrane effect produces greater depth to the resonant structures and the interconnected pores of the sample prevent the energy [30].

By contrast, there was no improvement at the low-medium frequencies for OPMF samples with 30 wt.% and 40 wt.% PU binder. Nevertheless, both samples were found to improve the absorption coefficient in the frequency range of 2500 Hz to 4500 Hz compared to pure OPMF without any binder. The acoustic performance of the OPMF with 30 wt.% PU is similar to the 40 wt.% PU, showing the maximum absorption coefficient at frequency 4150 Hz. The mechanism involved in sound absorption for these samples are still the same where the sound waves are dissipated through interaction (mechanical friction) occurred at the boundaries between PU binder and fibre. Although these samples are not favourable in terms of sound absorption performance compared to the other two preceding samples, the mechanical properties are slightly improved due to many pores are filled with a binder [11].

Table 2 tabulates the values of the sound absorption for OPMF samples in the octave bands frequency (250 Hz, 500 Hz, 1000 Hz and 2000 Hz), together with the noise reduction coefficient

(NRC). It was found that NRCs for all samples are above 0.5, thus indicating that OPMF is highly absorptive [31]. Of these samples, OPMF with 10 wt.% PU binder demonstrates the optimum value with the most significant increase of NRC at 0.66. As the binder content increases, the NRC of OPMF samples significantly drop. The NRC reduction is explained by the fact that adding more percentages of PU binder affect the physical properties and consequently give impact on the sound absorption.

TABLE 2 Effect of PU binder on noise reduction coefficient of OPMF

Sample OPMF with PU loading (wt.%)	Frequency (Hz)				NRC
	250	500	1000	2000	
0	0.11	0.39	0.94	0.88	0.58
10	0.21	0.64	0.92	0.86	0.66
20	0.17	0.47	0.98	0.77	0.60
30	0.15	0.40	0.92	0.86	0.58
40	0.13	0.35	0.92	0.85	0.56

Table 3 compares the NRC values of the optimum OPMF sample obtained from this study with the other type of natural fibres as well as synthetic fibres from previous research studies. OPMF with 10 wt.% PU binder improves NRC far effectively than other natural fibers such as corn, coir, grass, sugarcane and bamboo fibre. The sample, however, was found to be slightly 0.10 lower than the synthetic glass wool fibre. Nevertheless, this comparison indicates that the oil palm Mesocarp fiber with 10 wt.% binder is capable to be a good sound absorption panel when looking at the environmental, ecological and health effects of synthetic fibre.

TABLE 3 Noise reduction coefficient of OPMF and other type of fibres from previous research

Material	NRC	References
10wt.% PU/OPMF	0.66	-
Corn fibre	0.33	Fouladi et. al [32]
Coir fibre	0.40	Fouladi et. al [32]
Grass fibre	0.41	Fouladi et. al [32]
Sugarcane fibre	0.42	Fouladi et. al [32]
Bamboo	0.53	Koizumi et. Al [34]
Polyurethane	0.58	Bies and Hansen [35]
Glass wool	0.76	Bies and Hansen [35]

Analytical modelling

For sufficient acoustic material to be used as a porous absorber, it is desirable to predict acoustical absorption in function of frequency. To these days, there are many models available to predict the porous absorbent acoustic features which can save time and numerous trial experiments. In this research, the Delaney-Bazley model and Johnson-Champoux-Allard model

were employed to model the acoustic properties of the OPMF samples as per described in Sections 3.2 and 3.3, respectively. Figures 5–9 show the comparison between the analytical models and the measured absorption coefficient for samples OPMF used in this work. The predicted results of Delaney-Bazley model and Johnson-Champoux-Allard model follow closely the experimental result practically throughout the considered frequency range.

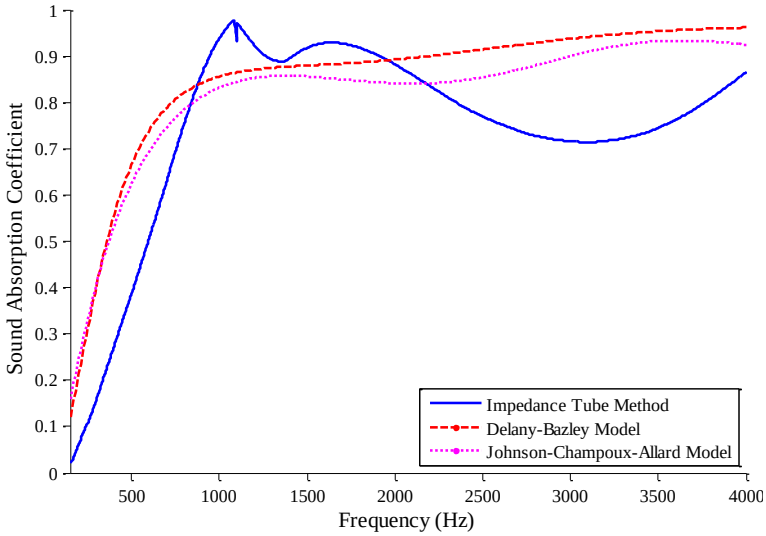

Figure 5. Comparison between the experimental results and predicton models for pure OPMF.

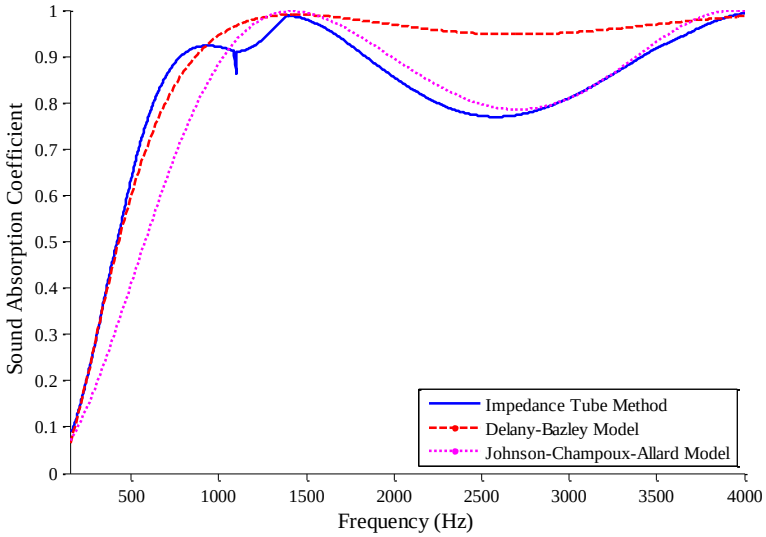

Figure 6. Comparison between the experimental results and predicton models for OPMF sample with 10 wt.% PU binder.

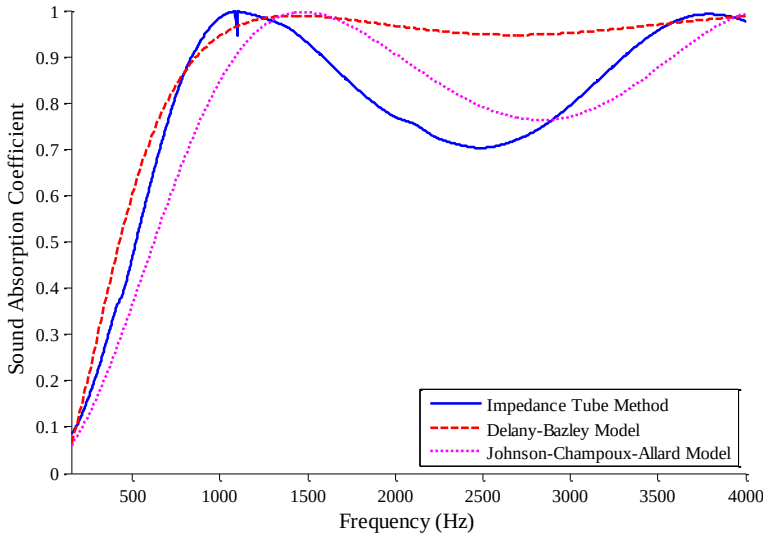

Figure 7. Comparison between the experimental results and predicton models for OPMF sample with with 20 wt.% PU binder.

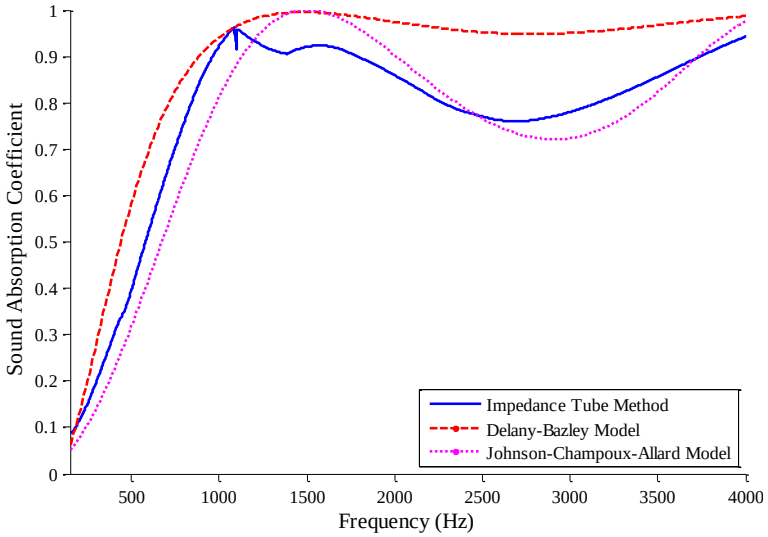

Figure 8. Comparison between the experimental results and predicton models for OPMF sample with with 30 wt.% PU binder.

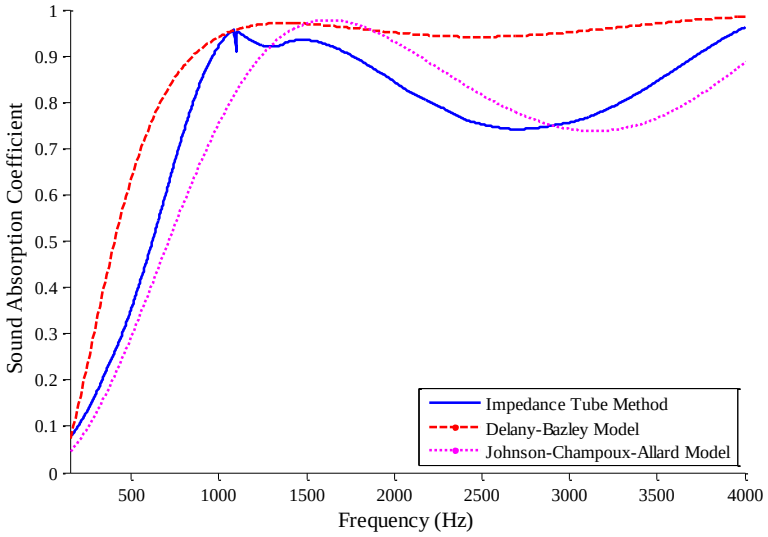

Figure 9. Comparison between the experimental results and predicton models for OPMF sample with with 40 wt.% PU binder.

From Figures 5–9, it can be seen that except pure OPMF, the Delaney-Bazley model predict the sound absorption of OPMF samples with PU binder well particularly in the frequency range less than 1500 Hz. However, the error becomes larger towards the medium to high-frequency range. The discrepancies of the prediction might be because the model is developed by a simple empirical approach and fast approximation using one parameter which is flow resistivity [32]. Despite this disadvantage, the Delaney-Bazley model has shown better prediction in the classical fibrous material where the porosity close to 1, for example, glass wool [30]. The glass wool normally has open pores where the connection from one pore to another pore is strong. According to Oliva and Hongisto [33], the Delaney-Bazley model is suitable for the low-frequency range and capable to give good results between 4000 Hz to 10000 Hz.

Meanwhile, the Johnson-Champoux-Allard model produces better sound absorption prediction compared to the previous model where it displays a similar pattern of spectra and fit to the acoustic behaviour of OPMF samples. It showed that the model was in agreement with the experimental results, thus proved the Johnson-Champoux-Allard model could be used successfully as an analytical tool for porous material such as OPMF. However, as the frequency and PU binder concentration increases, the position of the second peak was not properly estimated. Anomalies in the results may be due to the fact that the model does not take into account the binder used in the sample separately. In this case, the binder was assumed part of the fibres by cover their surfaces and filled the pore between them [32].

5. CONCLUSION

This work shows an investigation of oil palm mesocarp fibre and its acoustical performance. The influences of binder addition on the physical properties and the sound absorption coefficient of oil palm mesocarp were determined. In the study, the experiment was conducted by adopting an impedance tube method, while two analytical approaches were implemented to support the analyses, namely Delaney-Bazley model and Johnson-Champoux-Allard model. The experimental result shows that the OPMF sample with 10 wt.% of PU binder demonstrated the best acoustic performance in terms of noise reduction and sound absorption coefficients in most of the medium to high frequencies, although 20 wt.% PU binder displayed the highest sound absorption

coefficient of 0.99 at 1000 Hz. Moreover, by increasing binder concentration has shifted the maximum and minimum peaks toward low frequency. In terms of the prediction model, the Johnson-Champoux-Allard model had the advantage over Delaney-Bazley analytical model where it not only displayed a similar pattern of sound absorption but also predicted resonance peaks very well. The outcome of this research clearly shows the potential of oil palm mesocarp fibre as a promising material to be utilized as a sound absorber panel, and replace the use of synthetic materials. The work also can be served as a guide for future designing of effective porous absorbers.

ACKNOWLEDGEMENTS

The authors would like to acknowledge the Faculty of Mechanical and Manufacturing Engineering at the Universiti Tun Hussein Onn Malaysia (UTHM) for the use of their lab facilities and support, and the Ministry of Higher Education Malaysia for their financial support under Fundamental Research Grant Scheme (FRGS) vote 1546.

REFERENCES

[1] Malaysian oil palm statistics 2017 - 37th edition, Economics and Industry Development Division, MPOB, Malaysian Palm Oil Board, (2018).
[2] Singh P., Sulaiman O., Hashim R., Peng L. C., Singh R. P., Environment, Development and Sustainability vol **15**, issue 2 (2013) pp. 367-383.
[3] Shaari N. Z. K., Lye O. T., Ahmad S., Journal of Oil Palm Research vol **18** (2006) pp. 198-203.
[4] Kushairi A., Singh R., Ong-Abdullah M., Journal of Oil Palm Research vol **29** (2017) pp. 431-439.
[5] Sari N. H., Rahman A., Syafri E., International Journal of Nanoelectronics and Materials vol **12**, issue 2 (2019) pp. 193-204.
[6] Luangkiattikhun P., Tangsathitkulchai C., Tangsathitkulchai M., Bioresource Technology vol **99**, issue 5 (2008) pp. 986-997.
[7] Awalludin M. F., Sulaiman O., Hashim R., Nadhari W. N. A. W., Renewable and Sustainable Energy Reviews vol **50** (2015) pp. 1469-1484.
[8] Jansar K. N., Roslan A. M., Hassan M. A., Pertanika Journal of Scholarly Research Reviews vol **4**, issue 1 (2018) pp. 31-40.
[9] Zakaria M. R., Norrrahim M. N. F., Hirata S., Hassan M. A., Bioresource Technology vol **181** (2015) pp. 263-269.
[10] Idris S. S., Rahman N. A., Ismail K., Bioresource Technology vol **123** (2012) pp. 581-591.
[11] Yang H. S., Kim D. J., Lee Y. K., Kim H. J., Jeon J. Y., Kang C. W., Bioresource Technology vol **95**, issue 1 (2004) pp. 61-65.
[12] Berardi U., Iannace G., Building and Environment vol **94** (2015) pp. 840-852.
[13] Nor M. J. M., Ayub M., Zulkifli R., Amin N., Fouladi M. H., Journal of Applied Sciences vol **10**, issue 22 (2010) pp. 2887-2892.
[14] Maderuelo-Sanz R., Barrigon Morillas J. M., Martín-Castizo M., Gomez Escobar V., Rey Gozalo G., Latin American Journal of Solids and Structures vol **10**, issue 3 (2013) pp. 585-600.
[15] Borlea A., Rusu T., Ionescu S., Cretu M., Ionescu A., Romanian Journal of Acoustics and Vibration vol **8**, issue 2 (2011) pp. 95-98.
[16] Sambu M., Yahya M. N., Latif H. A., Zaman I., Ghazali M. I., International Review of Mechanical Engineering vol **10**, issue 4 (2016) pp. 284-288.

[17] Delany M. E., Bazley E. N., Applied Acoustics vol **3**, issue 2 (1970) pp. 105-116.
[18] Dunn I. P., Davern W. A., Applied Acoustics vol **19**, issue 5 (1986) pp. 321-334.
[19] Allard J., Atalla N., Propagation of sound in porous media: Modelling sound absorbing materials. United Kingdom: John Wiley & Sons, (2009).
[20] Champoux Y., Allard J. F., Journal of applied physics vol **70**, issue 4 (1991) pp. 1975-1979.
[21] Johnson D. L., Koplik J., Dashen R., Journal of fluid mechanics vol **176** (1987) pp. 379-402.
[22] Ballagh K. O., Applied Acoustics vol **48**, issue 2 (1996) pp. 101-120.
[23] Panneton R., Gros E., ACTA Acustica united with Acustica vol **91**, issue 2 (2005) pp. 342-348.
[24] Umnova O., Attenborough K., Shin H. C., Cummings A., Applied Acoustics vol **66**, issue 6 (2005) pp. 607-624.
[25] Kino N., Ueno T., Applied Acoustics vol **69**, issue 7 (2008) pp. 575-582.
[26] Luu H. T., Perrot C., Panneton R., ACTA Acustica united with Acustica vol **103**, issue 6 (2017) pp. 1050-1063.
[27] Kim K.-Y., Doh S. J., Im J. N., Jeong W. Y., An H. J., Lim D. Y., Fibers and Polymers vol **14**, issue 4 (2013) pp. 639-646.
[28] Latif H. A., Yahya M. N., Zaman I., Sambu M., Ghazali M. I., Hatta M. N. M., ARPN Journal of Engineering and Applied Sciences vol **11**, issue 4 (2016) pp. 2462-2466.
[29] Wang C. N., Torng J. H., Applied Acoustics vol **62**, issue 4 (2001) pp. 447-459.
[30] Garai M., Pompoli F., Applied Acoustics vol **66**, issue 12 (2005) pp. 1383-1398.
[31] Lee J., Kim G. H., Ha C. S., Journal of applied polymer science vol **123**, issue 4 (2012) pp. 2384-2390.
[32] Fouladi M. H., Ayub M., Nor M. J. M., Applied Acoustics vol **72**, issue 1 (2011) pp. 35-42.
[33] Oliva D., Hongisto V., Applied Acoustics vol **74**, issue 12 (2013) pp. 1473-1479.
[34] Koizumi T., Tsujiuchi N., Adachi A., In: High Performance Structures and Composites vol **59**, (2002) pp. 157-166.
[35] Bies D., Hansen C., Engineering Noise Control: Theory and Practice. New York, NY, USA: Taylor and Francis, (2009).